Morphological and elemental characterization of leaf-deposited particulate matter from different source types : a microscopic investigation

Reference:
Castanheiro Ana, Wuyts Karen, Hofman Jelle, Nuyts Gert, De Wael Karolien, Samson Roeland.- Morphological and elemental characterization of leaf-deposited particulate matter from different source types : a microscopic investigation
Environmental Science and Pollution Research - ISSN 0944-1344 - Heidelberg, Springer heidelberg, 28:20(2021), p. 25716-25732
Full text (Publisher's DOI): https://doi.org/10.1007/S11356-021-12369-Z
To cite this reference: https://hdl.handle.net/10067/1760820151162165141

Morphological and elemental characterization of leaf-deposited particulate matter from different source types: a microscopic investigation

Ana Castanheiro [1,*], Karen Wuyts [1], Jelle Hofman [1,2], Gert Nuyts [3], Karolien De Wael [3], Roeland Samson [1]

[1] Laboratory of Environmental and Urban Ecology, Department of Bioscience Engineering, University of Antwerp, Groenenborgerlaan 171, 2020 Antwerp, Belgium

[2] Solutions4IoT Lab, Imec, High Tech Campus 31, 5656 AE Eindhoven, The Netherlands (current address)

[3] Antwerp X-ray Analysis, Electrochemistry & Speciation (AXES), Department of Bioscience Engineering, University of Antwerp, Groenenborgerlaan 171, 2020 Antwerp, Belgium

* Corresponding author: Ana.Castanheiro@uantwerpen.be

Abstract

Particulate matter (PM) deposition on urban green enables the collection of source-specific particulate pollution from a diversity of contexts and insight into the physico-chemical profiles of PM is key for identifying main polluting sources. This study reports on the morphological and elemental characterization of $PM_{2\text{-}10}$ deposited on ivy leaves from five different environments (forest, rural, roadside, train, industry) in the region of Antwerp, Belgium. Ca. 40,000 leaf-deposited particles were thoroughly investigated by particle-based analysis using scanning electron microscopy coupled with energy-dispersive X-ray spectroscopy (SEM/EDX) and their physico-chemical characteristics were explored for PM source apportionment purposes. The size distribution of all deposited particles was biased towards small-sized PM, with 32% of the particles smaller than 2.5 µm ($PM_{2.5}$) and median diameters of 2.80 - 3.09 µm. The source type influenced both the particles' size and morphology (aspect ratio and shape), with roadside particles being overall the smallest in size and the most spherical. While forest and rural elemental profiles were associated with natural PM, the industry particles revealed the highest anthropogenic metal input. $PM_{2\text{-}10}$ profiles for roadside and train sites were rather comparable and only distinguishable when evaluating the fine (2 – 2.5 µm) and coarse (2.5 – 10 µm) PM fractions separately, which enabled the identification of a larger contribution of combustion-derived particles (small, circular, Fe-enriched) at the roadside compared to the train. Random Forest prediction model classified the source type correctly for 61% - 85% of the leaf-deposited PM. The still modest classification accuracy denotes the influence of regional background PM and demands for additional fingerprinting techniques to facilitate source apportionment. Nonetheless, the obtained results demonstrate the utility of leaf particle-based analysis to fingerprint and pinpoint source-specific PM, particularly when considering both the composition and size of leaf-deposited particles.

Keywords

Particulate matter • Leaf deposition • Ivy leaves • PM biomonitoring • SEM/EDX • Particle characterization • Source apportionment

Acknowledgments

The authors thank W. Dorriné for the valuable discussions on SEM/EDX analysis. A.C. acknowledges the Research Foundation Flanders (FWO) for her PhD fellowship (1S21418N).

1. Introduction

Ambient air pollution is a global public concern affecting practically all countries and parts of society, with nine out of ten people worldwide breathing air exceeding the World Health Organization (WHO) air quality guidelines (WHO 2018) and an estimated death toll of three million people every year (WHO 2016). Among air pollutants, particulate matter (PM) poses the greatest risk to human health (WHO 2015) due to their small inhalable size and association with hazardous constituents such as black carbon (BC) and metals (Anderson et al. 2012; Kampa and Castanas 2008; Scapellato et al. 2007; Terzano et al. 2010). Main constituents of PM include organic (OC) and black carbon (BC), ammonia (NH_4^+), nitrates (NO_3^-), sulfates (SO_4^{-2}), sea salt, mineral dust, and a diversity of trace elements associated with certain emission sources (Pacyna and Pacyna 2001; Putaud et al. 2004; Querol et al. 2001; Viana et al. 2008). While carbon emissions are mostly due to combustion processes (e.g. vehicle fuel combustion, biomass burning), NH_4^+/NO_3^-/SO_4^{-2} are typical secondary aerosol components derived from agriculture (NH_4^+), vehicle exhausts (NO_3^-) or industry (SO_4^{-2}) (Buekers et al. 2014; Viana et al. 2008). Sea spray comprises ions of Cl, Na, Mg, with elements Al, Si, K, Ca, Ti, Mn, Fe, being characteristic for soil dust contributions (Almeida et al. 2006; Vercauteren et al. 2011). Trace elements can be related to fuel combustion (e.g. Pb, V and Ni), non-exhaust traffic emissions such as from tire abrasion (Cu, Zn, Cd), brake pads (Cu) or vehicle corrosion (Fe, Cu, Zn, Cd, Cr) and incinerator or industrial emissions (Cu, Zn, Cd) (Pacyna and Pacyna 2001; Zhang et al. 2012). With a wide range in composition, PM is often grouped according to its aerodynamic diameter into PM_{10}, $PM_{2.5}$ and $PM_{0.1}$, for particles smaller than 10 µm (coarse PM), 2.5 µm (fine PM) and 0.1 µm (ultrafine PM), respectively. The size and composition of PM, as well as their number and surface area, are known to be key features in terms of their impact on human health (Anderson et al. 2012; Cassee et al. 2013; Kampa and Castanas 2008; Kelly and Fussel 2016; Kim et al. 2015; Künzli et al. 2000; Rivas et al. 2020).

Among other ecosystem services, urban vegetation has been regularly documented to intervene positively in the problem of atmospheric pollution by promoting the capture and deposition of PM (Escobedo et al. 2011; Grote et al. 2016; Janhäll 2015; Litschke and Kuttler 2008; Weber et al. 2014).

Green elements such as plant leaves are also valuable biological sensors for time-integrated exposure assessment of air and habitat quality (e.g., Baldacchini et al. 2017; Castanheiro et al. 2020; Grote et al. 2016; Hofman et al. 2017; Kardel et al. 2012; Mo et al. 2015; Sawidis et al. 2011). Leaf monitoring offers more rapid and cost efficient strategies to investigate PM than e.g. the conventional collection of air-pumped filters, thus, enabling for studies with high spatial resolution and at different levels (street/neighborhood/city/region). This is of particular relevance to investigate site-specific conditions of PM within typically heterogeneous urban settings, as particle size and chemical composition are known to vary considerably from source to source (Vercauteren et al. 2011). From a practical point of view, plants are relatively cheap, portable and adaptable, resilient to meteorological conditions, and require no electricity to sample the atmosphere in which they grow. Yet, more complex analyses using advanced chemical techniques require significant processing time and reduce the rapidity advantage of the biomonitoring approach relative to traditional PM monitoring. But still, these advanced techniques in biomonitoring can provide a bulk of data on PM characteristics.

To be able to use plant leaves as a monitoring tool for PM requires a comprehensive understanding of the features and mechanisms underlying PM deposition. Particle-based techniques, such as scanning electron microscopy coupled with energy-dispersive X-ray spectroscopy (SEM/EDX) applied at leaf level allows for a close-up look onto the typical predominant characteristics of PM. Although the application of SEM/EDX to investigate particles deposited onto leaves is not original (e.g., Baldacchini et al. 2017, 2019; Ottelé et al. 2010; Sgrigna et al. 2016), it is often limited in terms of particle number or land uses considered. The experiment of Ottelé et al. (2010) was rather dedicated to counting particles deposited onto common ivy, only describing the composition of three leaf-deposited particles. After washing *Quercus ilex* leaves, Sgrigna et al. (2016) analyzed the subsequent filters for a total of 100 particles per sample, overall up to 3,129 particles from two sampling locations at two heights. Baldacchini et al. (2019) considered a total of 200 leaf-deposited particles per *Quercus ilex* tree at seven locations within the same Italian urban forest. Yet, research on how many particles are necessary to properly represent the overall leaf-deposited particles is not available until now. To our knowledge, the application of SEM/EDX to characterize leaf-deposited PM emitted and/or present at distinct land uses or source types is still scarce, with the exception of the comparison of leaf-deposited particles at park and street sites by Baldacchini et al. (2017). The latter study, across 20 European cities from 18 countries, included sampling sites from distinct climates and background levels of pollution, which complicates further source apportionment besides the distinction between park and street conditions. The identification and characterization of specific PM sources might thus be better achieved by focusing on distinctive urban environments in a single city or region. Therefore, the present study reports on the morphological features and elemental composition of ca. 40,000 leaf-deposited particles on ivy (*Hedera sp.*) leaves collected from five source types (forest, rural, roadside, train, industry) in the region of Antwerp, Belgium. The main objectives were to investigate how morphological and elemental characteristics of leaf-deposited PM differed across different source types, and to assess the potential of leaf microscopic monitoring using SEM/EDX for source apportionment of PM. Whether the particles analyzed in this study were representative of the overall leaf-deposited particles, was also explored.

2. Materials and methods

2.1. Study area and leaf sampling

The province of Antwerp is the most populated region in Belgium, with ca. 1,845M inhabitants and a density of 644 inhabitants per km^2 (Flanders 2018). The city of Antwerp contains the second largest harbor in Europe and, consequently, has a prominent industrial area, being also characterized by high traffic intensity roads and highways. In order to investigate leaf-deposited PM under the influence of distinct environments and anthropogenic pressures, leaf samples were collected from five sites considered to be mainly exposed to different source types of pollution, namely, forest, rural, roadside, train and industry (Fig. S.1). The leaf samples collected in this study were previously analyzed for their magnetic enrichment and metal deposition (Castanheiro et al. 2016). Selected monitoring sites comprise background (Forest and Rural sites) and urban/suburban (Roadside, Train, Industry) environments that are typically present in urbanized and industrialized areas. The Forest and Rural sampling sites were located at Merksplas, ca. 37 km from Antwerp's city center to avoid the influence of road and railway traffic and industrial emissions. These sites were located 300 m apart in the same residential/rural area. The Forest site (51°21'22.44"N, 4°52'53.95"E) was located in a forested area, at 30 m distance from a low-traffic road, and the Rural site (51°21'13.21"N, 4°53'2.79"E) only 1 m away from a low-traffic road, considered the main local PM contributing source. The mentioned roads mostly serve the inhabitants of the small residential/rural neighborhood, resulting in low traffic intensities. The Roadside location (51°11'33.90"N, 4°25'19.80"E), on the other hand, was close to traffic lights and 7 m away from a busy road intersection, resulting in high traffic densities and a lot of stop-and-go traffic. The presence of tram lines, at 30 m distance, is considered to be of minor influence compared to the high road traffic intensity on site. The Train site (51° 9'35.47"N, 4°30'6.60"E) was in rural Boechout, only 5 m distant from a railway track and with negligible road traffic contribution. Finally, the Industry site (51° 9'52.41"N, 4°20'14.00"E) was situated in Hoboken, within a non-ferrous metal industrial complex, 4 m distant from a road with low/medium traffic intensity mostly used by the factory workers and for cargo loading/unloading. The main contributing source on site is related with the industrial processing and recycling of precious and other (non-ferrous) metals (e.g., Ag, Au, Pt, Se, Bi, Pb, Cu, Ni), with reported exceeding emissions of As, Cd and Pb (VMM 2017).

Leaves of common ivy (*Hedera sp.*) plants were sampled in spring 2014 (on March 27 and April 16), with a total of eight fully-developed undamaged leaves per test site. Ivy was selected as test species as it is widely spread in both natural and urban settings, and was present within all sampling locations. Ivy leaves were picked from the outer canopy of existing plants at 1.30 - 1.70 m above ground, in order to minimize the contribution of soil dust resuspension and to simulate human inhalation height. Although fully-developed leaves were targeted for sampling, the age of the collected leaf samples was not known, as this monitoring campaign was passive (i.e., collection of existing leaves). However, as this study looked into the characterization of site-specific, thus, source-dependent leaf-deposited particles, instead of quantifying their total accumulation level, we considered the uncertainty in leaf age to be of less relevance. No precipitation was registered during leaf sampling nor on the previous three days.

2.2. Scanning electron microscopy coupled with energy-dispersive X-ray spectroscopy (SEM/EDX)

The morphological and elemental characterization of leaf-deposited PM considered the deposition of particles on both leaf sides (abaxial and adaxial). For each collected ivy leaf, a circular sample with 1 cm in diameter (equivalent to ca. 79 mm^2 leaf surface area) was cut out using a metallic puncher. The leaf SEM samples were retrieved from the center of the leaf lamina avoiding the main veins. From the eight leaves per sampling site, four leaves were used to obtain adaxial (upper leaf side) samples and the remaining four leaves to obtain abaxial (lower leaf side) samples. Samples were dried at room temperature for a minimum of three days, prior to be carbon coated under vacuum. For SEM/EDX analysis, a field emission gun – environmental scanning electron microscope (FEG-ESEM) equipped with an EDX detector was employed (Quanta 250, FEI, USA; at AXES and EMAT research groups, University of Antwerp, BE). The operating parameters used were: 20 kV accelerating voltage, 10^{-4} Pa sample chamber pressure, 10 mm working distance, 3.6 spot size.

All leaf SEM samples (n = 40; 8 per sampling site, 4 adaxial and 4 abaxial) were examined for their deposited particles in a total surface area of ca. 6 mm^2 per leaf. The SEM/EDX analysis was automatized and computer controlled (CCSEM) using the INCA software (Oxford Instruments, UK) for feature detection and analysis. At the beginning of each SEM session, leaf samples were briefly explored using both secondary electron images (SEI) (Fig. 1, a) and backscattered electron images (BSE) (Fig. 1, b). While SEI show a three-dimensional perception of the surface being analyzed (leaf surface and leaf-deposited particles), BSE provide information on its chemical composition with bright, high *Z* elements (deposited particles) contrasting with the leaf background surface. The detection and analysis of leaf-deposited particles by CCSEM was performed in backscattered electron configuration (Baldacchini et al. 2019). For each leaf sample, the software-proposed feature detection was evaluated by comparing the secondary and backscattered electron images to ensure that all deposited particles (clearly visible in the SEI) were correctly detected at the BSE while organic components of the leaves (e.g., trichomes) were ignored and that particulate agglomerates were properly decomposed into their constituent particles. The feature thresholds of the backscattered electron detector signal (upper and lower gray level thresholds, related to the intensity of the detected signal) were adjusted, if needed, so that all features (i.e., individual deposited particles) within those thresholds were set to white and all others were set to black (Inca 2006) (Fig. 1, b). As the position and thickness of each leaf sample could affect the feature thresholds, this procedure of feature checking and adjusting of the thresholds was done for the first segmented fields of each sample.

The central area of each leaf sample was selected and automatically segmented into 50 fields with fixed dimensions of 414 µm × 285 µm each in a x-y plane. The software was set to analyze 20 particles (or features) per field, which delivered around 1,000 leaf-deposited particles for a total of 50 fields. The CCSEM scanned the particles "row-by-row", first within the x direction before proceeding in the y direction, and this occurred consecutively until a total of 20 particles were found within each field, before moving to the next field (Fig. 1, b). For the magnification used (500x), an interaction volume (i.e., the excitation volume under the sample surface as a result of the interaction with the electron beam (Marinello et al. 2008; Zhou et al. 2006)) equivalent to at least 1 µm in diameter was required to ensure that the deposited particles were correctly identified from the leaf surface and also recognizable from particle agglomerates. Given that the identification of leaf-deposited particles was computer controlled and not permanently assisted by a SEM operator, a more conservative minimum size threshold was chosen. Only particles with equivalent circular diameter (ECD; the diameter of a circle with the same area as the projected particle on the x-y plane (Xie et al. 2005), defined as the square root of (4xarea)/perimeter (Inca 2006)) equal or larger than 2 µm were considered. The particles' ECD obtained by SEM/EDX is defined as particle size diameter in the context of this study. No maximum particle size threshold was initially defined in the software, but particles with an ECD larger than 50 µm were disregarded from the data analysis.

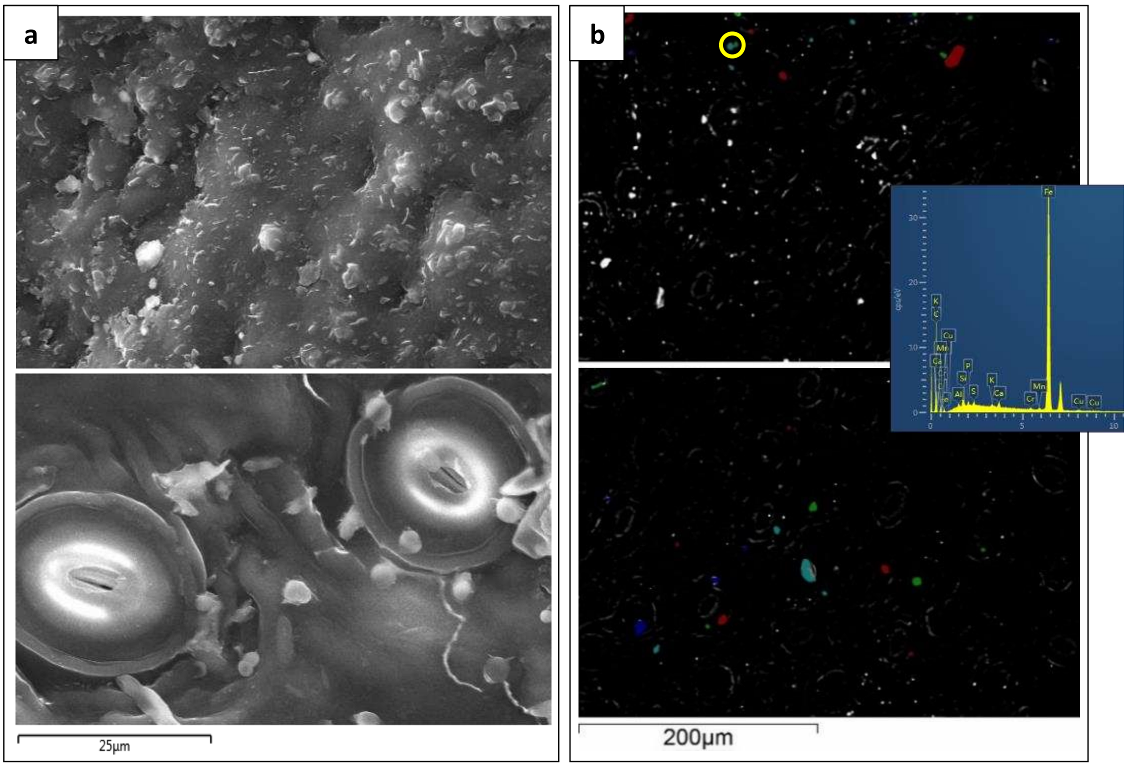

Fig. 1 *– Leaf-deposited PM on ivy: a) secondary electron images (SEI) of an adaxial (top) and an abaxial (bottom) leaf sample. Stomata are visible on the abaxial sample; b) backscattered electron images (BSE) of two fields scanned on the same sample. Deposited particles are visible as bright, white spots against a dark background, as the leaf surface is of organic nature (low Z). The colored particles (20 per field) correspond to the particles (features) selected for SEM/EDX analysis. These particles can represent a small fraction of the particles deposited in a field (top) or cover almost the totality of particles present (bottom). An illustrative particle EDX-spectrum is also shown.*

From the 40 leaf samples, a total of 39,409 leaf-deposited particles were analyzed by SEM/EDX. For each particle (*i*), the CCSEM mode delivered a range of parameters such as the field in which the particle was found with x and y coordinates within that field, as well as their morphological features (e.g., ECD, perimeter, area, aspect ratio, shape) and composition percentage C_{xi} (%, m/m) in terms of the relative weight of each element present (*x*). Chemical composition (C_{xi}) was obtained for elements with atomic number (*Z*) between 6 (C) and 93 (Np). As the leaf samples were carbon-coated and EDX is unable to correctly measure oxygen, elements C and O were disregarded from the obtained composition. A total of 64 chemical elements were considered, with Na, Mg, Al, Si, P, S, Cl, K, Ca, Fe, Cu and Pb being the overall main identified elements in the leaf-deposited particles. The aspect ratio and shape factor estimated by SEM/EDX are useful indicators for evaluating the morphology of deposited particles. The aspect ratio was automatically calculated as the ratio of maximum to minimum Feret diameter (i.e., dimensionless, as maximum and minimum Feret diameters consist of the furthest and shortest distance between any two parallel tangents on the particle) (Inca, 2006). The shape factor, calculated as the ratio of the square of the perimeter to 4π times the area, is a measure of roundness and circularity of the particles, considering both their form and roughness (Olson 2011; Pabst and Gregorova 2007; equation from Inca 2006). In the case of a spherical particle, its projection on the x-y plane is a circle, and the aspect ratio and shape are both equal to 1. For a particle with a morphology far from spherical, the aspect ratio and shape (also named circularity) are higher than the unity, with maximum values being obtained for the least circular and most angular particles. The average field (n = 50) coverage by the selected particles (20 per field) was obtained for each leaf sample using the y coordinates, in order to estimate the leaf surface area onto which these particles were deposited. This allowed to estimate the density of leaf-deposited particles, in number of particles per cm^2 of leaf surface. The leaf surface area of collected leaves was determined while they were fresh using a LI-3100C leaf area meter (Licor Biosciences, USA).

2.3. Data analysis

2.3.1. Data processing

The data obtained via SEM/EDX was initially handled and refined through a customized script-code developed in MATLAB (MathWorks, USA). Among others, the developed functions allowed for removing any incorrect particle entry (e.g., ECD > 50 µm), recalculating the composition C_{xi} after excluding O (C had been automatically excluded in the software), and calculating the weighted-volume composition percentage, $W\%_x$ (%, v/v). Two approximations were considered for the latter calculation step, namely, that particles were near-spherical in order to obtain their volume (v_i) (Equation 2.1) and that particles had constant density (Castanheiro et al. 2016; Baldacchini et al. 2017). This allowed to estimate the volume of each analyzed particle and to calculate the weighted-volume elemental composition. The weighted-volume composition in each element x ($W\%_x$) was obtained per source type (or leaf sample) by normalizing the composition percentage C_{xi} of all individual particles therein deposited (*n*) for their total particle volume (Equation 2.2). Errors associated with such approximations are assumed to be reduced, as a large number of particles were selected for analysis.

$$v_i = \frac{4\,\pi}{3} \cdot \left(\frac{ECD_i}{2}\right)^3 \qquad (2.1) \qquad\qquad W\%_x(\%, v/v) = \frac{\sum_{i=1}^{n} v_i . C_{xi}}{\sum_{i=1}^{n} v_i} \qquad (2.2)$$

2.3.2. Particle size distribution and chemical composition

Statistical analyses on the morphological and compositional data were performed using JMP Pro 14 (SAS Institute Inc., USA). The ranges of particle size reported along this study refer to the total particles (ECD 2 – 50 µm) and to the fraction $PM_{2\text{-}10}$ (ECD 2 – 10 µm). A distinction between fine PM (ECD 2 – 2.5 µm) and coarse PM (ECD 2.5 – 10 µm) was considered whenever relevant. Due to the large predominance of small-sized particles, the particle size and other morphological data were very negatively skewed, and no algebraic transformation resulted in a normal distribution. Mann-Whitney and Kruskal-Wallis tests were performed to investigate the influence of leaf side and source type, respectively, on the morphological characterization of the leaf-deposited particles, and Spearman's correlations for assessing the association between particle features. When site effects were significant, the characteristics of deposited particles between the various monitoring sites were compared using the post-hoc Steel-Dwass tests.

Additionally, the weighted-volume composition per source type were used to estimate the elemental mass of leaf-deposited particles (Equation 2.3). This was done by multiplying the weighted-volume percentages of leaf-deposited particles in each element ($W\%_x$) by the estimated total particle volume and by the corresponding solid-state density, D_x (i.e., atomic mass per volume, kg m^{-3}; values taken from www.webelements.com/periodicity/density/), following Baldacchini et al. (2019). This calculation included the particles deposited on both leaf sides, resulting in the mass of leaf-deposited particles in each element (M_x; µg). The total mass of analyzed leaf-deposited particles (M_p) was obtained by summing the M_x of all elements.

$$M_x = W\%_x \cdot \sum_{i=1}^{n} v_i \cdot D_x \qquad (2.3) \qquad\qquad PLI = \sqrt[m]{CF_{M1} \times CF_{M2} \times \ldots \times CF_{Mm}} \qquad (2.4)$$

Enrichment factors usually consider measured concentrations against values found in literature of a specific crustal earth element (e.g., Al) from a certain background-reference (Bourliva et al. 2017; Hsu et al. 2016; Ny and Lee 2010). However, this strategy may overlook local geochemical and lithological characteristics, as well as the influence of regional atmospheric dust (Reimann and Caritat 2000). Alternatively, the elemental enrichment in this study was calculated using the Forest site as a reference, by comparing the mass (M_x) of leaf-deposited particles at each site against those from the Forest (µg source type / µg Forest). The Forest site was selected as reference because it was the most isolated monitoring site in relation to anthropogenic point sources (e.g., roads), corroborated by the natural, rather than anthropogenic, elemental composition observed at the Forest leaf-deposited PM. The estimated enrichment factors correspond to mass concentration ratios against the Forest reference site, and can also be designated contamination factors. These values were then used to calculate the Tomlinson pollution load index (PLI, Tomlinson et al. 1980) to assess how much the metal content at the studied sites exceeded the metal content in the natural, background environment. The *PLI* is defined as the m-th root of the multiplication of contamination factors (CF_{Mm}), with CF_{Mm} here being the ratio of the content of each metal *M* (for *m* considered metals) to its background value at the forest site (Equation 2.4).

2.3.3. Representativeness of analyzed particles

The obtained morphological and elemental information were cumulative-averaged to evaluate how many particles were required to obtain a representative profile of the leaf-deposited particles at a certain condition (site, leaf side). This was done for some parameters of interest such as the particle size diameter and content in e.g., Si, Fe, Pb. The cumulative-averaged data were plotted against the number of analyzed particles (in the order in which they were scanned by the SEM/EDX) in order to estimate how many particles would be necessary to achieve stable, representative values.

2.3.4. Source apportionment

Principal component analysis (PCA) was performed on the (previously scaled) compositional C_{xi} (%, m/m) and morphological (ECD, aspect ratio, shape) data of leaf-deposited particles to identify groups of interrelated variables in an attempt to discriminate the investigated sites. The morphology and elemental composition of the analyzed particles, as well as the mass elemental enrichment, the *PLI* and the density of particles were examined across the different tested sites in an attempt to discriminate them. Finally, we used the Bootstrap Forest method, also known as Random Forest, to investigate the potential of SEM/EDX data for source apportioning the analyzed leaf-deposited PM. Random Forest (RF) is a powerful machine learning method for quantitative predictions and classification purposes, based on ranking input variables according to their importance for predicting the variable of interest (Breiman 2001; Peters et al. 2007; Philibert et al. 2013). The RF predicts a response value by averaging the predicted response across many decision trees, in which each tree is constructed on a bootstrap sample (i.e., a random sample of observations, drawn with replacement) of the training data. The training dataset, used to estimate the model and set on 60% of the entire data, was validated using 20% of the data (validation dataset), while the remaining 20% was used as a test dataset, for checking the prediction after the model was constructed. This strategy of randomly splitting the dataset into training, validation and test datasets is commonly used when an independent dataset for model evaluation is lacking (Breiman 2001; Peters et al. 2007). The morphology (size diameter, aspect ratio, shape) and composition (in major elements only) of particles (observations) were used as input variables to predict the probability of such observations belonging to the various sites (response). The observations were then classified into the source type for which its predicted probability was the highest. The classification accuracy (CA) was calculated per source type as the ratio of correctly classified observations (i.e. predicted source type that was actually correct) to the total of observations (Kononenko and Kukar 2007). The application of RF method was done using the Bootstrap Forest in JMP Pro 14.

3. Results and discussion

3.1. Representativeness of analyzed particles

The particles analyzed by SEM/EDX were checked for their representativeness potential of the monitoring sites in question, in terms of size diameter and composition C_{xi} (%,m/m) in Si (lithogenic/soil element) and Fe (soil-derived element, as well as traffic-indicator; Guevara 2016; Lorenzo et al. 2006; Querol et al. 2001; Vercauteren et al. 2011; Viana et al. 2008), and in Pb for the Industry site. Stable plateaus in both Si and Fe composition were found after ca. 600 and 1,000 analyzed particles for the Rural site, but constant values were not achieved for the Forest even after 7,000 particles (Fig. 2). For Roadside and Train, a more or less stable composition in Si was observed after 500 particles, while the Fe content hardly reached a stable plateau. When looking into the abaxial and adaxial leaf-deposited particles from the Industry leaves, the cumulative-averaged composition in Si and Fe reached a steadiness after ca. 500 particles, while the composition in Pb still increased with an increasing number of particles. The cumulative-averaged size diameter of particles reached stable values after 500 particles, with exception of the Forest site, which required at least 2,000 particles. The number of particles necessary to properly represent the tested parameters (size diameter, Si, Fe, Pb) and across the different sites was not consistent, but this should be in the order of a few hundreds of particles. According to our results, for most cases the application of SEM/EDX to about 500 to 1,000 particles would already deliver information representative of the leaf-deposited particles at each condition. As atmospheric PM consists of a mix of airborne particles with both local (specific) and regional (common) influences, the number of analyzed particles should be as high as possible to increase the reliability of results. When targeting specific fractions only (e.g., within a small particle size interval, or with a content above or below certain defined values), the required number of analyzed particles could be lower than in this study.

3.2. Leaf-deposited particles per source type

3.2.1. Particle size and morphology

From the total of 39,409 leaf-deposited particles analyzed by SEM/EDX, 95% (37,440 particles) had a particle size diameter (ECD) ≤ 10 µm (2 - 10 µm), i.e. belonging to the range of PM_{10}. The relative contribution of very coarse particles (> 10 µm) was most evident (11%) on the abaxial surface of ivy leaves exposed at the Rural site, but still negligible in the overall analyzed particles. The mean particle size diameter for the PM_{2-10} fraction was 3.52 ± 1.58 µm, with median values varying between 2.80 and 3.09 µm across the studied locations (Table 1). The particle size distribution was evidently biased towards the smaller particles. Around 50% of all leaf-deposited particles (i.e., for all tested sites and both leaf sides) had a diameter between 2 and 3 µm (Fig. 3, S.2). Furthermore, between 28% and 35% of the particles were smaller than 2.5 µm, thus belonging to the fraction of fine PM ($PM_{2.5}$). Particle diameter was significantly influenced by source type (Kruskal-Wallis, $p < 0.0001$): all monitored sites differed in particle size diameter with the exception for the comparisons Roadside-Industry, Forest-Train and Rural-Train (Steel-Dwass, $p > 0.12$) (Fig. S.3). Considering the particles deposited on both leaf sides, the median particle size followed the order RD = I (2.92 µm) < F (2.99 µm) < R (3.02 µm) < T (3.06 µm) (Table 1).

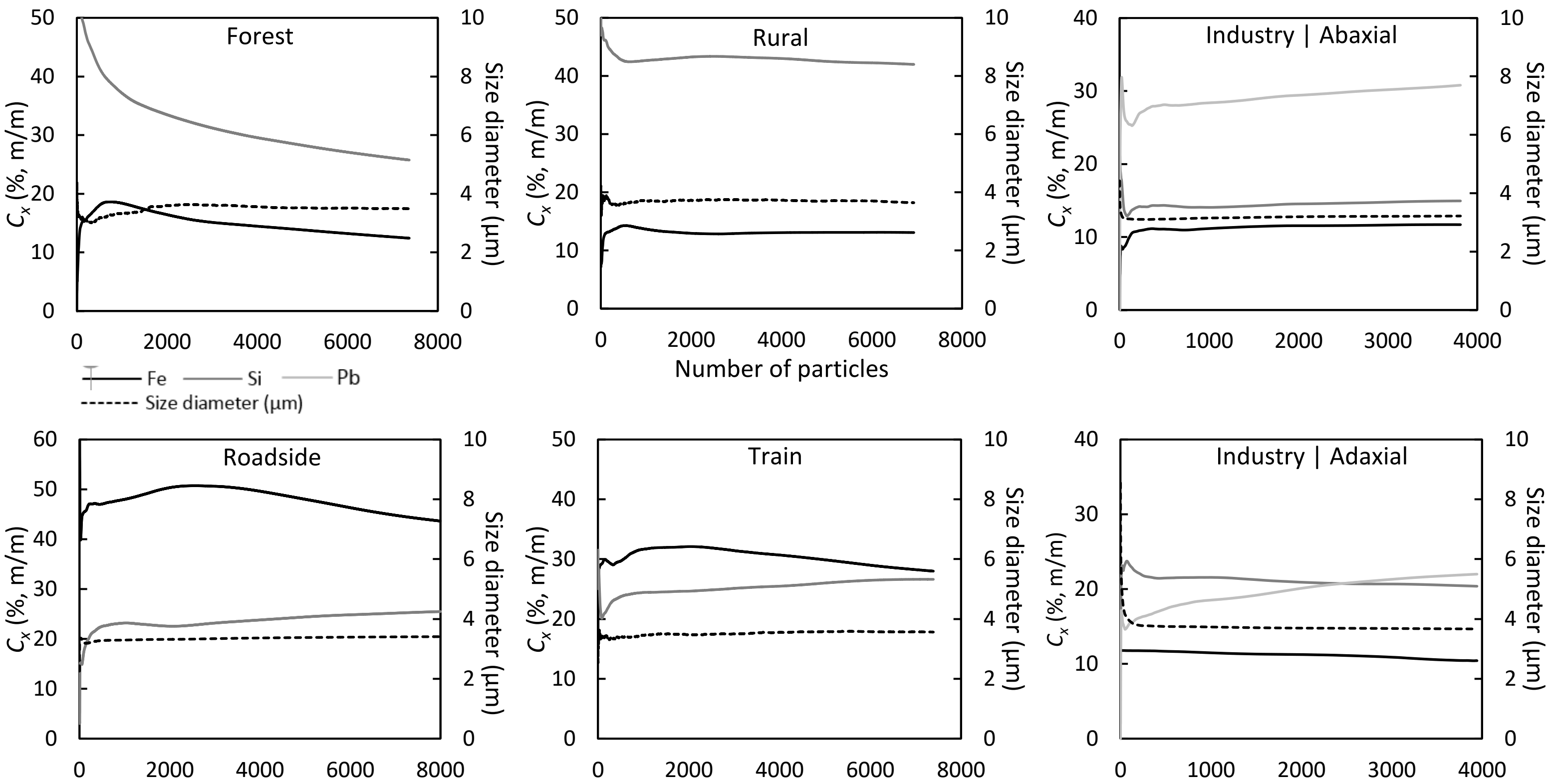

Fig. 2 *- Plots of cumulative-averaged composition C_{xi} (%, m/m) in Fe, Si and Pb, and size diameter of leaf-deposited particles ($PM_{2\text{-}10}$) per source type in function of the number of analyzed particles. Both adaxial and abaxial sides are included, except for the Industry site for which these data are shown separately.*

Table 1 *– Median size diameter (in µm), aspect ratio and shape (dimensionless) of leaf-deposited particles (N) per source type, considering both leaf sides (AB + AD), only the abaxial (AB) or the adaxial (AD) side. Sites not associated with the same letter within each line indicate significantly different median values (Steel-Dwass tests, $p < 0.05$).*

AB + AD	Forest	Rural	Roadside	Train	Industry
Size Diameter	2.99^{b}	3.02^{c}	2.92^{a}	3.06^{bc}	2.92^{a}
Aspect Ratio	1.54^{c}	1.51^{b}	1.49^{a}	1.52^{bc}	1.52^{b}
Shape	1.15^{b}	1.15^{b}	1.12^{a}	1.15^{b}	1.18^{c}
N	7,366	6,931	7,997	7,390	7,756
AB	Forest	Rural	Roadside	Train	Industry
Size Diameter	2.95^{b}	2.99^{bc}	2.92^{b}	3.06^{c}	2.80^{a}
Aspect Ratio	1.59^{c}	1.52^{b}	1.47^{a}	1.58^{c}	1.49^{a}
Shape	1.18^{d}	1.15^{c}	1.10^{a}	1.20^{e}	1.13^{b}
N	3,938	3,182	4,017	3,527	3,812
AD	Forest	Rural	Roadside	Train	Industry
Size Diameter	3.02^{bc}	3.09^{c}	2.88^{a}	3.02^{b}	3.02^{b}
Aspect Ratio	1.49^{ab}	1.50^{b}	1.51^{b}	1.47^{a}	1.55^{c}
Shape	1.13^{a}	1.16^{b}	1.15^{b}	1.11^{a}	1.24^{c}
N	3,428	3,749	3,980	3,863	3,944

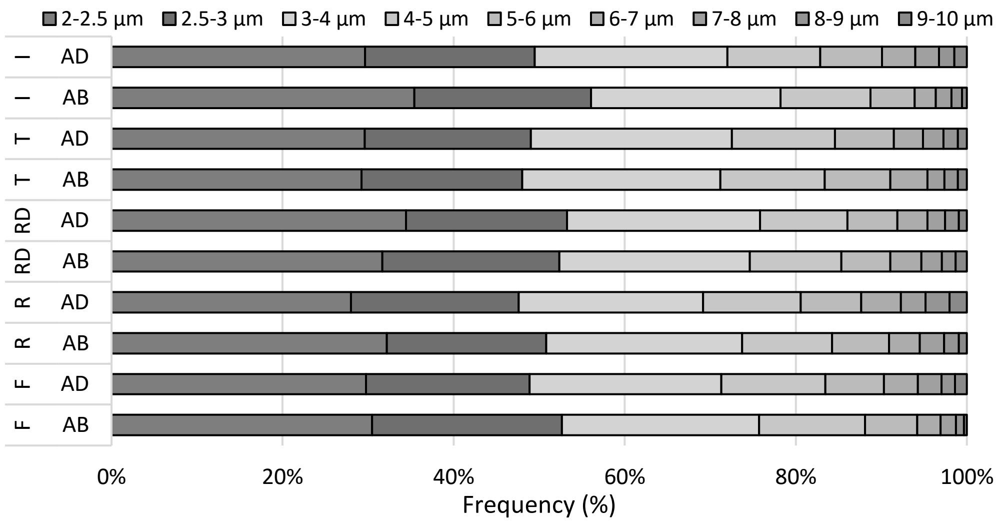

Fig. 3 *- Relative frequency of the particle size diameter (%) per source type (F - Forest, R - Rural, RD - Roadside, T - Train, I - Industry) and leaf side (AB – abaxial, AD – adaxial), in unit size bins from 2 to 10 µm, with an additional discrimination done for the particle size diameter of 2.5 µm, the upper limit of fine PM ($PM_{2.5}$).*

Leaf-deposited particles are often considered spherical or with a circular shape (as in e.g. Baldacchini et al. (2017, 2019), Castanheiro et al. (2016), Sgrigna et al. (2016), and in this study) to simplify quantitative composition calculations. However, atmospheric particles encompass a variety of shapes and geometries. The aspect ratio of the leaf-deposited particles ranged from 1.05 to 14.73. The closest the aspect ratio is to unity, the less elongated is the particle. Both symmetric and circular-like shapes are characterized by aspect ratios close to 1 (Olson 2011). Aspect ratio estimates are not applicable to extremely elongated particles such as fibers (aspect ratio > 5) though, but this was a minority (0.12%) in our study. Despite the variety of particle morphologies, the median aspect ratio was between 1.47 and 1.59 for all monitored sites and both leaf sides (Table 1). The median particle shape varied between 1.10 and 1.24 for all tested conditions (Table 1), with values ≈ 1 indicating circular particles (Pabst and Gregorova 2007). The morphology of the leaf-deposited particles, in both their aspect ratio and shape, was site-dependent ($p < 0.0001$). Leaf-deposited particles from Roadside were overall the most circular and less elongated, suggesting a high contribution of combustion-related particles such as iron oxides at this site (Breed et al. 2002; Conner et al. 2001; González et al. 2018; Peters et al. 2016; Piña et al. 2000). Spherical particles are typically indicative of high-temperature processes such as combustion (domestic, vehicle or industrial) and metal-mechanical industrial activities such as smelting (Conner et al. 2001; González et al. 2018). The morphology of particles was significantly different in terms of aspect ratio between the Roadside and Industry, and between those and the Forest site. In terms of shape, differences were also observed between Roadside and Industry, while Forest, Rural and Train were alike. The fact that the particles' shape differed between Roadside and Industry sites suggests that high-temperature processes (e.g. combustion, smelting) were of less relevance at the Industry, although it consists of a metal recycling plant, than at the Roadside. Median aspect ratio was highest for Forest (1.54), while median shape was highest for Industry (1.18).

The size distribution of particles deposited on both leaf sides was comparable in terms of magnitude (Fig. 3), but the median particle size differed significantly between both surfaces for three out of the five tested sites (Table 2). For Forest, Rural and Industry, the particle size was larger ($p < 0.0004$) on the adaxial than on the abaxial side. The aspect ratio and shape of particles were also dependent on leaf side, but no consistent trend was observed across all source types. The median aspect ratio was significantly smaller (closer to unity, thus, indicating less elongated particles) on the adaxial side of Forest, Rural and Train leaves compared to the abaxial side, while the opposite was observed for the Roadside and Industry (Table 2). Similar results were obtained regarding the shape of leaf-deposited particles, with exception for the Rural site, where particles on the abaxial side had a smaller shape factor, thus, were more circular, than those on the adaxial side. Considering the particles deposited on the abaxial side of ivy, median size diameter varied between 2.80 µm (Industry) and 3.06 µm (Train), aspect ratio between 1.47 (Roadside) and 1.59 (Forest), and shape between 1.10 (Roadside) and 1.20 (Train). For the adaxial side, the median particle size varied between 2.88 µm (Roadside) and 3.09 µm (Rural), with the lowest and highest aspect ratio and shape for, respectively, the Train (1.47; 1.11) and Industry (1.55; 1.24) sites. The morphology of the particles appeared to be influenced by the particle diameter, as larger particles were also more elongated and less circular (Fig. 4). This was transversal to all tested source types (Fig. S.4), and confirmed by significant positive correlations between particle size diameter and morphology (Spearman's, $p < 0.0001$), with correlation coefficients (ρ) of 0.15 to 0.24 between the diameter and aspect ratio, and of 0.45 to 0.56 between the diameter and shape of the particles. Both aspect ratio and shape parameters fluctuated in the same direction, with ρ of 0.65 to 0.73.

Table 2 *- Median size diameter (in µm), aspect ratio and shape (dimensionless) of leaf-deposited particles per source type, considering the particles deposited either on the abaxial (AB) or adaxial (AD) leaf side. For each site, significant differences (Mann-Whitney, p < 0.01) between abaxial and adaxial are shown with the larger value in bold.*

Source type	Forest		Rural		Roadside		Train		Industry	
Leaf side	AB	AD	AB	AD	AB	AD	AB	AD	AB	AD
Size Diameter	2.95	**3.02**	2.99	**3.09**	2.92	2.88	3.06	3.02	2.80	**3.02**
Aspect Ratio	**1.59**	1.49	**1.52**	1.50	1.47	**1.51**	**1.58**	1.47	1.49	**1.55**
Shape	**1.18**	1.13	1.15	**1.16**	1.10	**1.15**	**1.20**	1.11	1.13	**1.24**

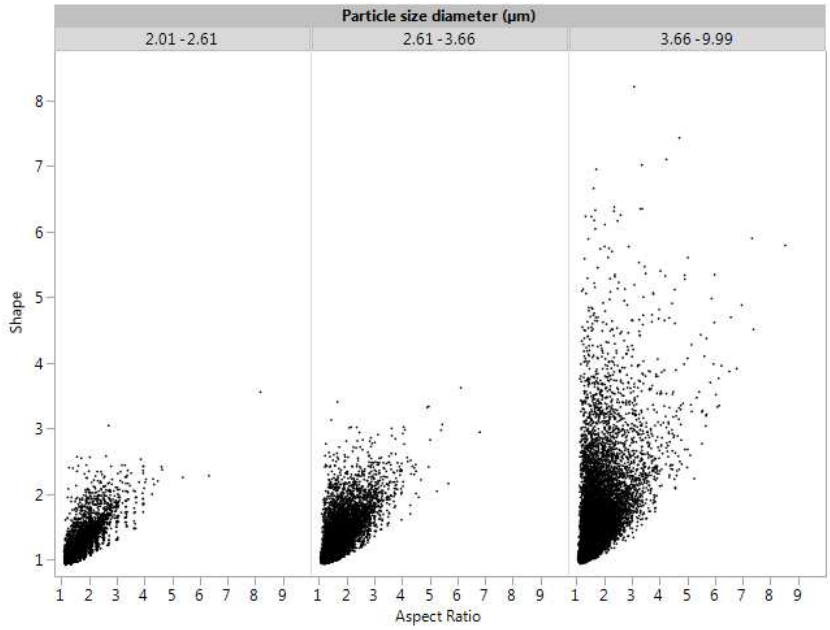

Fig. 4 – *Scatterplot of the aspect ratio (x axis) and shape (y axis) of all analyzed leaf-deposited $PM_{2\text{-}10}$, according to their size diameter subdivided in three equal intervals.*

3.2.2. Particle elemental composition

The elements most contributing to the overall composition of leaf-deposited particles were Si, Fe, Ca, S, K, Al, Pb, Cl, Na, Mg, P and Cu, which were also the most frequently identified elements (in addition to As; Table S.1). PM typically include, amongst others, crustal matter (Si, Ca, K, Al, Na, Mg, Fe, Ti, Mn), sea salt (Na, Cl, Mg) and traffic-derived compounds (e.g., Fe, Cr, Mn, Cu, Pb) (Amato et al. 2009; Vercauteren et al. 2011). The influence of the source type on the composition profiles ($W\%_x$) of the analyzed particles was investigated in terms of major and trace elements (Fig. 5), as they can point towards main polluting sources. The leaf-deposited particles from the Forest were mainly composed of Si, Ca, S, K, Fe, Al, Na and Cl. The major elements on the Rural site were Si, Ca, Al, Fe, Mg, K and for which Si had the highest relative contribution (ca. 45%) amongst all tested sites. Both Roadside and Train leaf-deposited particles had a comparable composition with Si and Fe as predominant elements, followed by Ca and Al. The highest Fe content, of ca. 24%, was observed for these two source types. The composition profile from Industry was remarkably different, with 30% of the particles composed of Pb and 5% of Cu, while these elements were negligible across the other sites. Trace elements such as As, Te, Zn, Sn, Sb also reached their highest concentrations for the Industry site, but minimal for the other sites. Although the relative elemental composition (%, m/m) varied per site (Table 3), all study sites were still under the influence of similar regional PM as they are located in the same region. Therefore, certain elements that are recognized as PM source indicators were found to be highly correlated ($p < 0.01$) independently of the source type, such as Na and Cl ($\rho = 0.29 – 0.82$, I < R < RD < T < F) and Si and Al ($\rho = 0.36 – 0.75$, R < RD < I < T < F) (Table S.2), associated with sea salt and crustal matter, respectively.

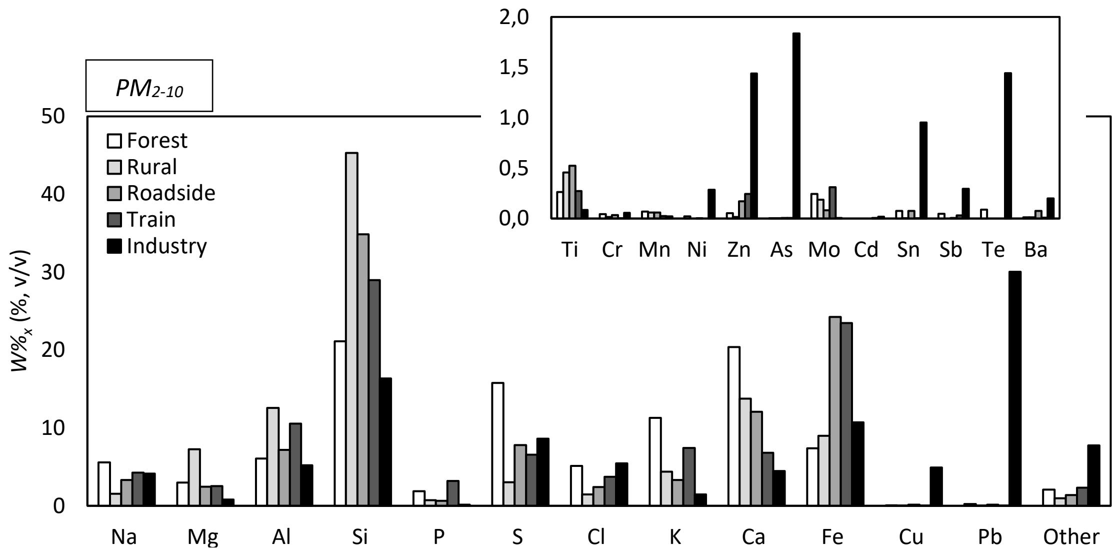

Fig. 5 *– Weighted-volume percentages (%, v/v) of major and trace (inset) elements quantified on the leaf-deposited particles (PM_{2-10}) by SEM/EDX. Major elements are responsible for > 92% of the overall composition, while trace elements include elements contributing to > 0.5% or metals commonly investigated in environmental studies. The class "Other" includes all remaining elements not considered major elements, i.e. including the trace elements shown in the inset. The composition profiles are presented per source type and include the particles deposited on both leaf sides. Discrimination between abaxial and adaxial leaf sides can be found in Fig. S.5.*

The Forest site was the least enriched in anthropogenic elements (Fig. 5), given the reduced traffic and industrial emissions nearby. The elemental enrichment at the traffic and industry sites compared to the Forest, thus used as a reference, can help assessing the importance of anthropogenic contributions across the remaining sites. Roadside particles were moderately enriched in Fe, Cu, Zn, As and Ba, while Train particles were moderately enriched in Fe, Zn and As (Table S.3). For Roadside, the enrichment level in As and Ba was considered significant within the fine and coarse PM, respectively. Leaf-deposited particles from Industry were enriched in trace elements Sb, Sn, Ni, Ba and Te, very highly enriched in Zn and extremely enriched in Cu, Pb and As. The highest elemental enrichment (4,734 µg / µg Forest) was observed for Pb content in the fine fraction of Industry particles. Also remarkable was the significant Pb-enrichment of the fine particles at both Roadside (13.4 µg/ µg Forest) and Train (12.1 µg/ µg Forest) sites, while the enrichment was negligible within the corresponding coarse fractions. The Tomlinson *PLI* including metals Fe, Cu, Pb (major elements), Ti, Cr, Mn, Ni, Zn, As, Mo, Cd, Sn, Sb, Te and Ba (trace elements), confirmed the Industry site as the highest polluted in terms of anthropogenic metal input. According to Qiao et al. (2013), degrees of pollution based on the Tomlinson *PLI* are defined as: $0 < PLI \leq 1$ unpolluted, $1 < PLI \leq 2$ moderately polluted, $3 < PLI \leq 4$ very highly polluted. Leaf-deposited particles from the Industry site even surpassed the highest defined *PLI* category, with a *PLI* of 6.8 and 7.5 for the fine and coarse PM fractions, respectively. The Rural and Train sites can be considered unpolluted, while the Roadside is considered polluted, particularly for the small particles. The Roadside *PLI* was 1.2 for the particles between 2.5 and 10 µm, and 1.7 for the particles between 2 and 2.5 µm.

Table 3 *– Mean elemental composition (%, m/m; major elements) of leaf-deposited particles across the five source types, considering particles deposited on both leaf sides (AB + AD). Sites not associated with the same letter within each line indicate significantly different median values (Steel-Dwass tests, p < 0.05).*

AB + AD	Forest	Rural	Roadside	Train	Industry
Na	4.4^{c}	1.6^{a}	3.6^{c}	4.5^{b}	3.4^{b}
Mg	2.9^{c}	6.5^{d}	2.1^{b}	2.4^{c}	0.8^{a}
Al	5.8^{a}	12.0^{e}	6.2^{c}	9.8^{d}	6.2^{b}
Si	19.0^{a}	39.4^{e}	27.5^{d}	26.4^{c}	17.0^{b}
P	2.2^{d}	1.1^{c}	0.5^{b}	3.8^{e}	0.1^{a}
S	15.9^{e}	4.5^{a}	7.5^{c}	6.9^{b}	8.5^{d}
Cl	3.6^{b}	1.4^{a}	2.6^{b}	3.5^{b}	4.4^{c}
K	16.2^{e}	5.7^{c}	2.9^{b}	9.6^{d}	1.8^{a}
Ca	18.9^{e}	13.6^{d}	9.8^{c}	6.9^{b}	3.7^{a}
Fe	8.3^{a}	12.6^{b}	35.3^{d}	23.4^{c}	11.6^{b}
Cu	0.1^{a}	0.1^{a}	0.2^{b}	0.0^{a}	5.8^{c}
Pb	0.0^{ab}	0.0^{a}	0.1^{b}	0.1^{ab}	29.4^{c}

The composition of atmospheric particles is not independent of their morphology and size, and vice-versa (Marcazzan et al. 2001). Instead, the aforementioned particle characteristics greatly depend on the emission sources, posing also different risks to human health (Bernstein et al. 2004; Daellenbach et al. 2020; EPA 2009; Guevara 2016; Kim et al. 2015; Schwarze et al. 2006). In this context, the elemental profiles revealed two key findings when discriminating between the fine (2 – 2.5 µm) and coarse (2.5 – 10 µm) deposited PM (Fig. 6). First, coarse PM was more enriched in Si compared to fine PM (especially for Rural and Roadside, with values 26% and 42% higher for the coarse PM compared to the fine PM). Second, fine particles from the Roadside were 72% more enriched in Fe than its coarse fraction, while the relative concentrations of all other elements were comparable between fine and coarse size ranges, and the site ordering was not altered (e.g., for Ca the order Forest > Rural > Roadside > Train > Industry was similar for the fine, coarse and total PM fractions). As larger particles contribute more to the estimated weighted-volume percentages ($W\%_x$), the overall composition profile (PM_{2-10}) (Fig. 5) is very similar to the profile of coarse PM (Fig. 6). However, the inclusion of smaller-sized particles (which are also the most health-concerning; Schwarze et al. 2006) may reveal useful relationships for the process of source apportionment. Fe is simultaneously a crustal matter constituent and an important indicator for road traffic and industrial activities (Vercauteren et al. 2011). More specifically, Fe is emitted by combustion processes (e.g. road exhaust emissions, industrial activities) and mechanical wear or abrasion (e.g. road non-exhaust emissions such as brake and tire wear, road pavement and rail friction), resulting in, respectively, fine and coarse Fe-rich particles (Amato et al. 2009; Lorenzo et al. 2006; Qadir et al. 2014; Viana et al. 2008). Coarse leaf-deposited particles from Roadside and Train were equally enriched in Fe (and the highest contribution across the five sites), suggesting similar wear or abrasion-related particle emissions. This enrichment greatly increased for the fine particles of Roadside, whereas it remained constant for the fine particles of Train. The larger contribution of smaller Fe-based particles in Roadside compared to Train reveals the influence of combustion processes, which are certainly present on the first location (high intensity car traffic) but variable on the second one, as both electrical- and diesel-powered trains may be passing at the Train site. As shown in this case, considering both the composition and the size of particles can aid in disclosing site or source type influences.

The abaxial vs. adaxial elemental profiles of PM_{2-10} showed comparable trends for the Rural site, whereas the leaf side seemed more relevant for the other source types (Table S.4). Particles deposited on the adaxial side were overall more enriched in Fe compared to the abaxial side, whereas the contrary was observed for S, K and Ca (Fig. S.5). The highest leaf side differences were observed in the mentioned elements for the Forest. For Roadside and Train, the weighted-volume composition in Fe was, respectively, 51% and 62% higher for the particles deposited on the adaxial side than on the abaxial side. This leaf-side influence occurred for both fine and coarse fractions at these two source types (Fig. S.6). A distinction between the lower-Fe abaxial contributions due to soil dust and the higher-Fe traffic contributions (more combustion-related at Roadside compared to Train) on the adaxial side is suggested by our results. This possibility, however, was not reflected on the particles' size. Large particles indicate crustal matter origin (Almeida et al. 2006), but the particle size diameter was not significantly different between the two leaf sides only for Roadside and Train (§3.2.1). The abaxial Fe content at these two sites was still higher than at the other sites, confirming the input of anthropogenic Fe emissions.

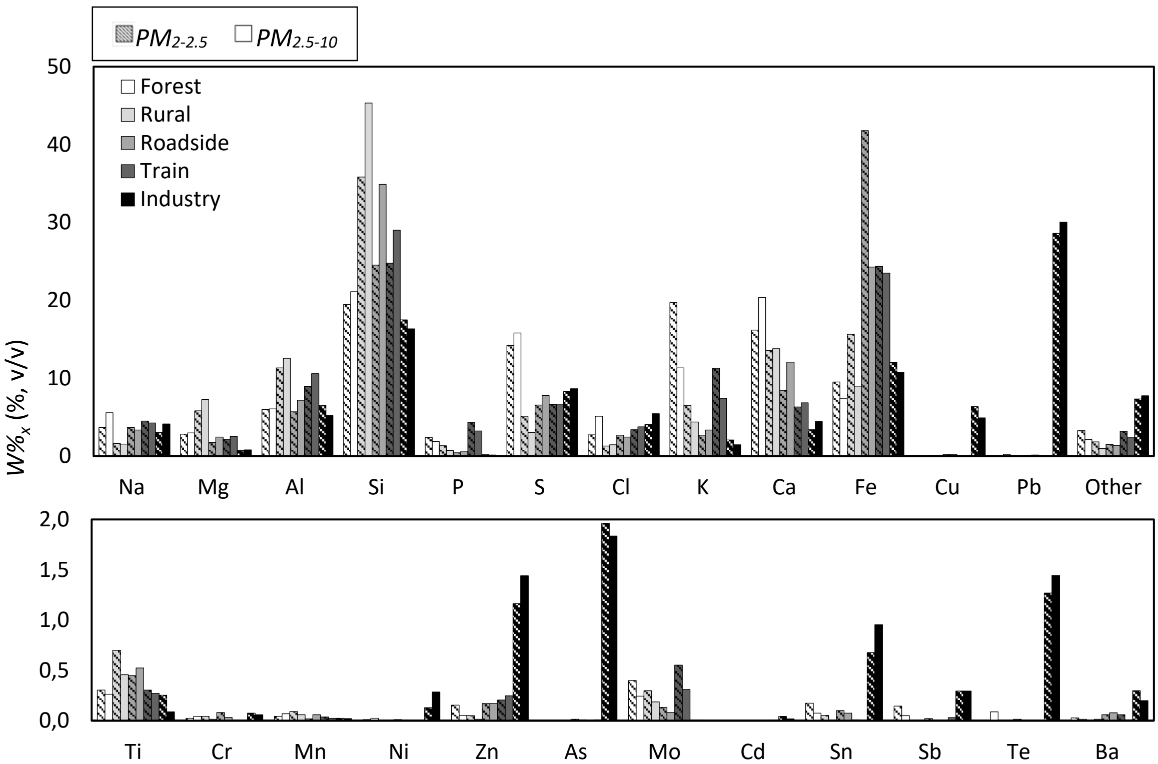

Fig. 6 *– Weighted-volume percentages (%, v/v) of major (top) and trace (bottom) elements quantified on the leaf-deposited fine PM (2-2.5 µm; bars with diagonal lines) and coarse PM (2.5-10 µm; solid bars). Major elements are responsible for > 92% of the overall composition, while trace elements include elements contributing to > 0.5% or metals commonly investigated in environmental studies. The class "Other" includes all remaining elements not considered major elements, i.e. including the trace elements. The composition profiles are presented per source type and include the particles deposited on both leaf sides.*

3.2.3. Particle mass and number

The total mass of leaf-deposited particles (of all analyzed particles; M_p) in the PM_{2-10} fraction was highest for Industry (181.5 µg), followed by the Roadside (111.2 µg), Train (102.8 µg), Rural (85.1 µg) and Forest (64.7 µg) (Fig. S.7). The contribution of finer particles to the total mass varied between 4.2% and 6.3% depending on the source type, with Roadside having the highest contribution of fine PM. The calculated mass does not refer to the total number of deposited particles on the collected ivy leaves, but to a fraction of it, namely to about 1,000 particles with diameter of 2 µm to 10 µm, that were analyzed per leaf sample. Given the large number of particles (ca. 7,000 per site), these estimates still provide an idea about the PM mass load across the test sites. As the number of analyzed particles was comparable across the investigated sites, and with a distribution similarly biased towards the smallest-sized particles, the calculated masses might rather be an indication of composition. The Industry site with the highest presence of metallic, higher *Z* elements, which often have high solid state density values (e.g., Pb = 11,340 kg m^{-3}), had also the highest calculated mass of leaf-deposited particles.

The density of leaf-deposited PM_{2-10} particles per source type was, on average, 32, 54, 34, 54 and 154 $\times 10^3$ particles cm^{-2}, for Forest, Rural, Roadside, Train and Industry, respectively. The estimated particle densities are somewhat lower than the ca. 100 to 200 $\times 10^3$ particles cm^{-2} ($PM_{2.5-10}$) observed by Baldacchini et al. (2019) on 8-months old *Quercus ilex* leaves, while they are rather comparable with the values measured on 5-months old *Platanus x acerifolia* across 20 European locations (Baldacchini et al. 2017). In the latter, particle densities mainly varied between 5 and 212 $\times 10^3$ $PM_{2.5-10}$ particles cm^{-2}, while the density of particles with a size diameter between 0.3 and 0.6 µm was up to 4 $\times 10^6$ particles cm^{-2}. The particle density of leaf-deposited particles depends on several factors, such as sampling site, exposure period and plant species, as species with different leaf macro- and micro-morphological characteristics can capture PM differently (Castanheiro et al. 2020; Dzierżanowski et al. 2011; Muhammad et al. 2019). Taking into account the total leaf surface area, the number of deposited particles ranged on average between 1.2 $x10^6$ (Forest) and 3.7 $x10^6$ (Industry) particles per leaf side of ivy. Main differences in particle density across leaf samples (n = 8) were observed for Rural, Train and Industry (Fig. S.8). The minimum and maximum estimated number of deposited particles was 0.7 and 10.5 $x10^6$, respectively for Forest and Industry, and both on the abaxial leaf side.

Ivy leaves present similar micro-morphology on both leaf sides (epicuticular wax structure defined as platelets and a comparable trichome density) with exception of the stomatal density, as stomata are only present on the abaxial side (Castanheiro et al. 2020). These stomatal openings on the lower leaf epidermis are often associated with enhanced accumulation of atmospheric particles (Sawidis et al. 2011). Several studies have shown that larger accumulation of PM occurs on the adaxial side of leaves compared to the abaxial side (Baldacchini et al. 2017; Ottelé et al. 2010; Shi et al. 2017; Wang et al. 2015). Despite of the few leaf replicates (four samples from each leaf side, per study site), the results of this study appear to support those findings. The particle density was significantly higher ($p = 0.03$) on the adaxial leaf side than on the abaxial side for two out of the five test sites (Rural and Industry).

3.2.4. Source apportionment of leaf-deposited particles

Principal component analysis (PCA) on the most representative elements (Na, Mg, Al, Si, P, S, Cl, K, Ca, Fe, Cu, Pb; %, m/m) and morphological parameters highlighted some correlated elements across the investigated sites, such as Na-Cl and Al-Si (Fig. 7). The main discriminant components (PC1 and PC2) explain 34.4% of the total variance within the particles' elemental composition (Fig. 7, a). PC1 discriminates particles based on the interrelated K, Ca, P, and S elements, in trade off with Al-Si composition and Fe. PC2 reflects the variation due to the correlated elements Na and Cl and, to a lesser extent, the composition in Cu and Pb. When including particle size diameter, aspect ratio and shape, PC1 and PC2 explain only 28.5% of the variance. Yet, the major elements are still grouped in the same way (Fig. 7, b). The aspect ratio and shape of leaf-deposited particles vary in the same direction, as corroborated by positive correlations between those parameters. This direction is opposed to that of Fe, supporting the observation that Fe-enriched particles were specifically more connected to less elongated and more circular morphologies, than the other considered elements. The size diameter of particles on its turn showed to be positively related with Na and Cl. The PCA biplots on the particles' morphology and composition did not reveal overall evident discrimination between the various source types. Yet, the Rural site is depicted to be more linked with elements Si and Al, the Roadside with Fe, and the Industry with Pb and Cu.

When performing the PCA separately on the particles deposited either on the abaxial or on the adaxial side, approximately the same groups of interrelated variables are identified (Fig. 7, c, d) with a few exceptions to mention. For instance, the abaxial leaf-deposited particles do not show a positive relationship between Na-Cl and the size of particles anymore (Fig. 7, c). The composition in Na and Cl of the adaxial particles appears rather associated with P, S and Ca, than with the particle size (Fig. 7, d). Still regarding the adaxial particles, Fe-enriched particles are strongly oppositely related with the size, shape and aspect ratio, corroborating again that Fe-rich particles tend to be particularly smaller and more circular compared to particles rather enriched in the other major elements. Traffic-derived combustion emissions generate small Fe-rich spherules, whilst coarse, non-spherical particles are also emitted from abrasion/corrosion of e.g. vehicle tires and brake pads (Matzka and Maher 1999). When making the distinction between coarse ($PM_{2.5-10}$) and fine ($PM_{2-2.5}$) particles (Fig. S.9), the key observation from the PCA is that coarse Fe-particles are more interrelated with Si and Al in comparison with the fine Fe-particles, suggesting coarse Fe-derived particles to be more associated with crustal matter dust than the fine fraction.

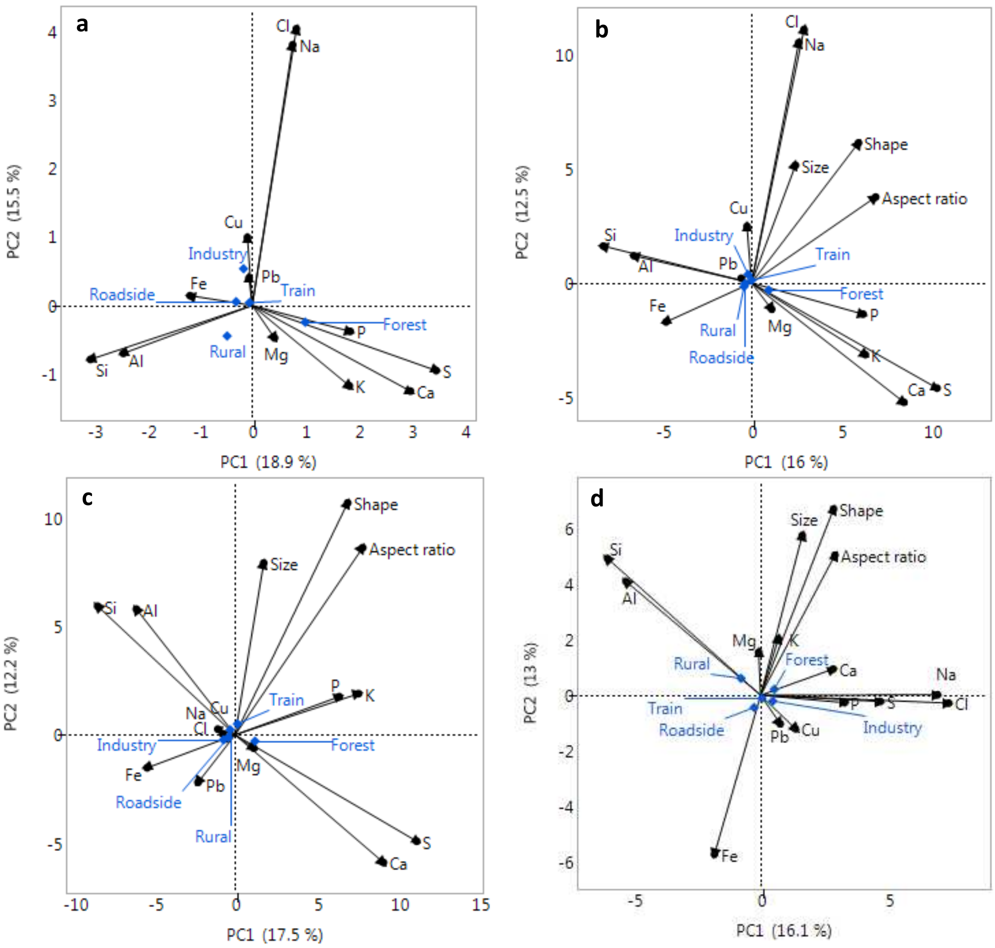

Fig. 7 *- Biplots of the first two components (PC1 and PC2) of a PCA considering as input variables a) the major elements (Na, Mg, Al, Si, P, S, Cl, K, Ca, Fe, Cu, Pb; %, m/m) of leaf-deposited particles, and b) the morphological parameters (size diameter, aspect ratio and shape) in addition to the major elements. The biplots of PCA a) applied separately to the abaxial (c) and adaxial (d) leaf-deposited particles are shown. Source types (in blue) are depicted from the PCA scores of the particles; given the large number of particles, the PCA scores are not shown to improve readability.*

According to the Bootstrap Forest, averaged over a total of 28 decision trees in the forest (the prediction model did not improve by including more trees), the input variables (size diameter, aspect ratio, shape, Na, Mg, Al, S, P, Si, Cl, K, Ca, Fe, Cu, Pb) yielded a satisfactory prediction of the source type, with a generalized R^2 of 0.83 (maximum is 1 for perfect models) and a misclassification rate of 0.28 for the training dataset (and ca. 0.33 for the validation and test datasets). The root mean square error (RMSE) and mean absolute deviation were still considerable, of 0.55 and 0.49, respectively. The smaller the latter values are, the better fits they indicate. From the 15 predictor variables, the composition was more accountable for splits in the decision trees than the morphological parameters, with the main split contributors being K, Pb, Fe, Ca, S and Si (Table S.5). This indicates that the content in these elements aid the most in correctly classifying the tested source types. On contrary, the diameter, aspect ratio and shape of particles, together with their content in Na and Cl, had the least discriminatory power. The first is likely because particles' size and morphology were comparably diversified across the five tested sites, while the second reflects the regional influence, rather than site-specific influence, of sea salt. The still modest classification accuracy of the RF model (61% - 85%) (Table 4) seems to denote a high influence of regional background PM across the monitored sites (Subramanian et al. 2007; van Dingenen et al. 2004; Viana et al. 2008). In some cases, regional PM can even dominate urban background PM levels, with urban PM emission sources contributing less than 15% (Keuken et al. 2013). In our study, the source apportionment of leaf-deposited PM based on the RF method was most efficient for Industry and Forest, as these sites were highly associated with Pb and K (main model predictors), respectively.

Table 4 *– Confusion matrix of predicted to actual observations, for the training dataset, with indication of classification accuracy (CA) per source type.*

	Predicted					
Actual	Forest	Rural	Roadside	Train	Industry	**CA**
Forest	3480	325	210	464	20	77%
Rural	436	2480	704	425	45	61%
Roadside	348	474	3409	360	131	72%
Train	666	417	461	2833	65	64%
Industry	55	142	442	86	3983	85%

4. Conclusions

Our results demonstrate that leaf particle-based analysis allows to fingerprint and pinpoint different source types, particularly when considering both the composition and size of leaf-deposited PM. Particles' size and morphology (aspect ratio and shape) were influenced by source type, with Roadside particles being overall the smallest in size and the most spherical. The median particle size followed the order Roadside = Industry < Forest < Rural < Train. The size diameter of deposited particles was evidently biased towards small-sized PM, with ca. 32% of all particles smaller than 2.5 µm ($PM_{2.5}$) and was larger on the adaxial leaf side than on the abaxial for two out of the five monitored sites. While Forest and Rural elemental profiles were mainly associated with natural PM (Si, Ca, S, K, Al, Mg, Na, Cl), the Industry particles revealed the highest anthropogenic metal input, particularly in Zn, Cu, Pb and As. The PM_{2-10} profiles for Roadside and Train were rather comparable and dominated by Si, Fe, Ca and Al. Discrimination between Roadside and Train samples was only possible by evaluating their fine (2 – 2.5 µm) and coarse (2.5 – 10 µm) PM characteristics. The fine particles from the Roadside were 72% more enriched in Fe than its coarse fraction, whereas this size-dependent enrichment was negligible for the Train, suggesting thus a larger contribution of combustion-derived particles (small, rather circular, Fe-enriched) at the Roadside compared to the Train site.

Using the particles' morphological and compositional information as input variables yielded a rather good RF prediction model, with K, Pb and Fe as main predictors. The source apportionment of leaf-deposited PM based on the RF model was most accurate for predicting Industry and Forest particles. The still modest classification accuracy of the RF model (61% - 85%) implies the rather high contribution of regional background PM. Moreover, this observation also demands for additional fingerprinting techniques that may aid in apportioning local PM sources more accurately.

5. Declarations

Ethics approval and consent to participate: Not applicable.

Consent for publication: Not applicable.

Availability of data and materials: The datasets used and/or analyzed during the current study are available from the corresponding author on reasonable request.

Competing interests: The authors declare that they have no competing interests.

Funding: A.C. received a PhD fellowship (1S21418N) from the Research Foundation Flanders (FWO) during the analysis and interpretation of data.

Authors' contributions: AC – methodology, formal analysis and investigation, writing - original draft preparation, reviewing and editing; KW – formal analysis, writing - review and editing; JH – writing - review and editing; GN – methodology, writing - review and editing; KW – conceptualization, supervision, resources, writing - review and editing; RS - conceptualization, supervision, resources, writing - review and editing. All authors read and approved the final manuscript.

6. References

Anderson, J.O., Thundiyil, J.G., Stolbach, A., 2012. Clearing the Air: A Review of the Effects of Particulate Matter Air Pollution on Human Health. Journal of Medical Toxicology. https://doi.org/10.1007/s13181-011-0203-1

Almeida, S.M., Pio, C., Freitas, M.C., Reis, M.A., Trancoso, M.A., 2006. Approaching PM2.5 and PM2.5-10 source apportionment by mass balance analysis, principal component analysis and particle size distribution. Science of the Total Environment 368, 663–674. https://doi.org/10.1016/j.scitotenv.2006.03.031

Amato, F., Pandolfi, M., Viana, M., Querol, X., Alastuey, A., Moreno, T., 2009. Spatial and chemical patterns of PM10 in road dust deposited in urban environment. Atmospheric Environment 43, 1650–1659. https://doi.org/10.1016/j.atmosenv.2008.12.009

Anderson, J.O., Thundiyil, J.G., Stolbach, A., 2012. Clearing the air: A review of the effects of particulate matter air pollution on human health. Journal of Medical Toxicology 8, 166–175. https://doi.org/10.1007/s13181-011-0203-1

Baldacchini, C., Castanheiro, A., Maghakyan, N., Sgrigna, G., Verhelst, J., Alonso, R., Amorim, J.H., Bellan, P., Bojović, D.Đ., Breuste, J., Bühler, O., Cântar, I.C., Cariñanos, P., Carriero, G., Churkina, G., Dinca, L., Esposito, R., Gawroński, S.W., Kern, M., Le Thiec, D., Moretti, M., Ningal, T., Rantzoudi, E.C., Sinjur, I., Stojanova, B., Aničić Urošević, M., Velikova, V., Živojinović, I., Sahakyan, L., Calfapietra, C., Samson, R., 2017. How does the amount and composition of PM deposited on *Platanus acerifolia* leaves change across different cities in Europe? Environmental Science & Technology 51, 1147–1156. https://doi.org/10.1021/acs.est.6b04052

Baldacchini, C., Sgrigna, G., Clarke, W., Tallis, M., Calfapietra, C., 2019. An ultra-spatially resolved method to quali-quantitative monitor particulate matter in urban environment. Environmental Science and Pollution Research 26, 18719–18729. https://doi.org/10.1007/s11356-019-05160-8

Bernstein, J.A., Alexis, N., Barnes, C., Bernstein, I.L., Nel, A., Peden, D., Diaz-Sanchez, D., Tarlo, S.M., Williams, P.B., Bernstein, J.A., 2004. Health effects of air pollution. Journal of Allergy and Clinical Immunology 114, 1116–1123. https://doi.org/10.1016/j.jaci.2004.08.030

Bourliva, A., Christophoridis, C., Papadopoulou, L., Giouri, K., Papadopoulos, A., Mitsika, E., Fytianos, K., 2017. Characterization, heavy metal content and health risk assessment of urban road dusts from the historic center of the city of Thessaloniki, Greece. Environmental Geochemistry and Health 39, 611–634. https://doi.org/10.1007/s10653-016-9836-y

Breed, C.A., Arocena, J.M., Sutherland, D., 2002. Possible sources of PM10 in Prince George (Canada) as revealed by morphology and in situ chemical composition of particulate. Atmospheric Environment 36, 1721–1731. https://doi.org/10.1016/S1352-2310(01)00500-3

Breiman, L., 2001. Random Forests. Machine Learning 45, 5–32.

Buekers, J., Deutsch, F., Veldeman, N., Janssen, S., Panis, L.I., 2014. Fine atmospheric particles from agricultural practices in Flanders: From emissions to health effects and limit values. Outlook on Agriculture 43, 39–44. https://doi.org/10.5367/oa.2014.0153

Cassee, F.R., Héroux, M.E., Gerlofs-Nijland, M.E., Kelly, F.J., 2013. Particulate matter beyond mass: Recent health evidence on the role of fractions, chemical constituents and sources of emission. Inhalation Toxicology 25, 802-812. https://doi.org/10.3109/08958378.2013.850127

Castanheiro, A., Hofman, J., Nuyts, G., Joosen, S., Spassov, S., Blust, R., Lenaerts, S., De Wael, K., Samson, R., 2020. Leaf accumulation of atmospheric dust: Biomagnetic, morphological and elemental evaluation using SEM, ED-XRF and HR-ICP-MS. Atmospheric Environment 221, 117082. https://doi.org/10.1016/j.atmosenv.2019.117082

Castanheiro, A., Samson, R., De Wael, K., 2016. Magnetic- and particle-based techniques to investigate metal deposition on urban green. Science of the Total Environment 571, 594–602. https://doi.org/10.1016/j.scitotenv.2016.07.026

Conner, T.L., Norris, G.A., Landis, M.S., Williams, R.W., 2001. Individual particle analysis of indoor, outdoor, and community samples from the 1998 Baltimore particulate matter study. Atmospheric Environment 35, 3935–3946. https://doi.org/10.1016/S1352-2310(01)00191-1

Daellenbach, K.R., Uzu, G., Jiang, J., Cassagnes, L.-E., Leni, Z., Vlachou, A., Stefenelli, G., Canonaco, F., Weber, S., Segers, A., Kuenen, J.J.P., Schaap, M., Favez, O., Albinet, A., Aksoyoglu, S., Dommen, J., Baltensperger, U., Geiser, M., El Haddad, I., Jaffrezo, J.-L., Prévôt, A.S.H., 2020. Sources of particulate-matter air pollution and its oxidative potential in Europe. Nature 587, 414–419. https://doi.org/10.1038/s41586-020-2902-8

Dzierżanowski, K., Popek, R., Gawronska, H., Sæbø, A., Gawroński, S.W., 2011. Deposition of particulate matter of different size fractions on leaf surfaces and in waxes of urban forest species. International Journal of Phytoremediation 13, 1037–1046. https://doi.org/10.1080/15226514.2011.552929

Escobedo, F.J., Kroeger, T., Wagner, J.E., 2011. Urban forests and pollution mitigation: Analyzing ecosystem services and disservices. Environmental Pollution 159, 2078-2087. https://doi.org/10.1016/j.envpol.2011.01.010

EPA, 2009. Integrated science assessment for particulate matter (final report). United States Environmental Protection Agency, Washington, DC. EPA/600/R-08/139F, 2009.

González, L.T., Longoria-Rodríguez, F.E., Sánchez-Domínguez, M., Leyva-Porras, C., Acuña-Askar, K., Kharissov, B.I., Arizpe-Zapata, A., Alfaro-Barbosa, J.M., 2018. Seasonal variation and chemical composition of particulate matter: A study by XPS, ICP-AES and sequential microanalysis using Raman with SEM/EDS. Journal of Environmental Sciences (China) 74, 32–49. https://doi.org/10.1016/j.jes.2018.02.002

Guevara, 2016. Emissions of primary particulate matter. In: Airborne particulate matter - sources, atmospheric processes and health. Issues in Environmental Science and Technology No. 42, pp. 1-26. The Royal Society of Chemistry, Cambridge.

Grote, R., Samson, R., Alonso, R., Amorim, J.H., Cariñanos, P., Churkina, G., Fares, S., Thiec, D. Le, Niinemets, Ü., Mikkelsen, T.N., Paoletti, E., Tiwary, A., Calfapietra, C., 2016. Functional traits of urban trees: Air pollution mitigation potential. Frontiers in Ecology and the Environment 14, 543–550. https://doi.org/10.1002/fee.1426

Hofman, J., Maher, B.A., Muxworthy, A.R., Wuyts, K., Castanheiro, A., Samson, R., 2017. Biomagnetic monitoring of atmospheric pollution: A review of magnetic signatures from biological sensors. Environmental Science & Technology 51, 6648–6664. https://doi.org/10.1021/acs.est.7b00832

Hsu, C.Y., Chiang, H.C., Lin, S.L., Chen, M.J., Lin, T.Y., Chen, Y.C., 2016. Elemental characterization and source apportionment of PM10 and PM2.5 in the western coastal area of central Taiwan. Science of the Total Environment 541, 1139–1150. https://doi.org/10.1016/j.scitotenv.2015.09.122

Inca, 2006. Inca Energy operator manual, issue 2.1. Oxford Instruments Analytical, UK.

Janhäll, S., 2015. Review on urban vegetation and particle air pollution – Deposition and dispersion. Atmospheric Environment 105, 130–137. https://doi.org/10.1016/J.ATMOSENV.2015.01.052

Kampa, M., Castanas, E., 2008. Human health effects of air pollution. Environmental Pollution 151, 362–367. https://doi.org/10.1016/j.envpol.2007.06.012

Kardel, F., Wuyts, K., Khavanin Zadeh, A.R., Wuytack, T., Babanezhad, M., Samson, R., 2012. Comparison of leaf saturation isothermal remanent magnetisation (SIRM) with anatomical, morphological and physiological tree leaf characteristics for assessing urban habitat quality. Environmental Pollution 183, 96–103. https://doi.org/10.1016/j.envpol.2012.11.030

Kelly, F. J., Fussel, J. C., 2016. Health effects of airborne particles in relation to composition, size and source. In: Airborne particulate matter - sources, atmospheric processes and health. Issues in Environmental Science and Technology No. 42, pp. 344-382. The Royal Society of Chemistry, Cambridge.

Keuken, M.P., Moerman, M., Voogt, M., Blom, M., Weijers, E.P., Röckmann, T., Dusek, U., 2013. Source contributions to PM2.5 and PM10 at an urban background and a street location. Atmospheric Environment 71, 26–35. https://doi.org/10.1016/j.atmosenv.2013.01.032

Kim, K.-H., Kabir, E., Kabir, S., 2015. A review on the human health impact of airborne particulate matter. Environment International 74, 136–143. https://doi.org/10.1016/j.envint.2014.10.005

Kononenko, I., Kukar, M., 2007. Machine Learning Basics, in: Machine Learning and Data Mining. Elsevier, pp. 59–105. https://doi.org/10.1533/9780857099440.59

Litschke, T., Kuttler, W., 2008. On the reduction of urban particle concentration by vegetation a review. Meteorologische Zeitschrift 17, 229–240. https://doi.org/10.1127/0941-2948/2008/0284

Lorenzo, R., Kaegi, R., Gehrig, R., Grobéty, B., 2006. Particle emissions of a railway line determined by detailed single particle analysis. Atmospheric Environment 40, 7831–7841. https://doi.org/10.1016/j.atmosenv.2006.07.026

Marcazzan, G., Vaccaro, S., Valli, G., Vecchi, R., 2001. Characterisation of PM10 and PM2.5 particulate matter in the ambient air of Milan (Italy). Atmospheric Environment 35, 4639–4650. https://doi.org/10.1016/S1352-2310(01)00124-8

Marinello, F., Bariani, P., Savio, E., Horsewell, A., De Chiffre, L., 2008. Critical factors in SEM 3D stereo microscopy. Measurement Science and Technology 19, 065705. https://doi.org/10.1088/0957-0233/19/6/065705

Mo, L., Ma, Z., Xu, Y., Sun, F., Lun, X., Liu, X., Chen, J., Yu, X., 2015. Assessing the capacity of plant species to accumulate particulate matter in Beijing, China. PLoS ONE 10, e0140664. https://doi.org/10.1371/journal.pone.0140664

Muhammad, S., Wuyts, K., Samson, R., 2019. Atmospheric net particle accumulation on 96 plant species with contrasting morphological and anatomical leaf characteristics in a common garden experiment. Atmospheric Environment 202, 328–344. https://doi.org/10.1016/j.atmosenv.2019.01.015

Ny, M.T., Lee, B.-K., 2010. Size distribution and source identification of airborne particulate matter and metallic elements in a typical industrial city. Asian Journal of Atmospheric Environment 4, 9–19. https://doi.org/10.5572/ajae.2010.4.1.009

Olson, E., 2011. Particle shape factors and their use in image analysis-Part 1: Theory. Journal of GXP Compliance 15, 85–96.

Ottelé, M., van Bohemen, H.D., Fraaij, A.L.A., 2010. Quantifying the deposition of particulate matter on climber vegetation on living walls. Ecological Engineering 36, 154–162. https://doi.org/10.1016/j.ecoleng.2009.02.007

Pabst, W., Gregorova, E., 2007. Characterization of particles and particle systems. ICT Prague 27-29.

Pacyna, J.M., Pacyna, E.G., 2001. An assessment of global and regional emissions of trace metals to the atmosphere from anthropogenic sources worldwide. Environmental Reviews 9, 269–298. https://doi.org/10.1139/er-9-4-269

Peters, J., Baets, B. De, Verhoest, N.E.C., Samson, R., Degroeve, S., Becker, P. De, Huybrechts, W., 2007. Random forests as a tool for ecohydrological distribution modelling. Ecological Modelling 207, 304–318. https://doi.org/10.1016/J.ECOLMODEL.2007.05.011

Peters, T.M., Sawvel, E.J., Willis, R., West, R.R., Casuccio, G.S., 2016. Performance of passive samplers analyzed by computer-controlled scanning electron microscopy to measure PM10-2.5. Environmental Science and Technology 50, 7581–7589. https://doi.org/10.1021/acs.est.6b01105

Philibert, A., Loyce, C., Makowski, D., 2013. Prediction of N2O emission from local information with Random Forest. Environmental Pollution 177, 156–163. https://doi.org/10.1016/J.ENVPOL.2013.02.019

Piña, A.A., Villaseñor, G.T., Fernández, M.M., Luszczewski Kudra, A., Leyva Ramos, R., 2000. Scanning electron microscope and statistical analysis of suspended heavy metal particles in San Luis Potosi, Mexico. Atmospheric Environment 34, 4103–4112. https://doi.org/10.1016/S1352-2310(99)00526-9

Putaud, J.P., Raes, F., Van Dingenen, R., Brüggemann, E., Facchini, M.-C., Decesari, S., Fuzzi, S., Gehrig, R., Hüglin, C., Laj, P., Lorbeer, G., Maenhaut, W., Mihalopoulos, N., Müller, K., Quass, U., Rodriguez, S., Schneider, J., Spindler, G., Brink, H. ten, Tørseth, K., Wiedensohler, A., 2004. A European aerosol phenomenology—2: chemical characteristics of particulate matter at kerbside, urban, rural and background sites in Europe. Atmospheric Environment 38, 2579–2595. https://doi.org/10.1016/J.ATMOSENV.2004.01.041

Qadir, R.M., Schnelle-Kreis, J., Abbaszade, G., Arteaga-Salas, J.M., Diemer, J., Zimmermann, R., 2014. Spatial and temporal variability of source contributions to ambient PM10 during winter in Augsburg, Germany using organic and inorganic tracers. Chemosphere 103, 263–273. https://doi.org/10.1016/j.chemosphere.2013.12.015

Qiao, Q., Huang, B., Zhang, C., Piper, J.D.A., Pan, Y., Sun, Y., 2013. Assessment of heavy metal contamination of dustfall in northern China from integrated chemical and magnetic investigation. Atmospheric Environment 74, 182–193. https://doi.org/10.1016/j.atmosenv.2013.03.039

Querol, X., Alastuey, A., Rodriguez, S., Plana, F., Ruiz, C.R., Cots, N., Massagué, G., Puig, O., 2001. PM10 and PM2.5 source apportionment in the Barcelona Metropolitan area, Catalonia, Spain. Atmospheric Environment 35, 6407–6419. https://doi.org/10.1016/S1352-2310(01)00361-2

Reimann, C., De Caritat, P., 2000. Intrinsic flaws of element enrichment factors (EFs) in environmental geochemistry. Environmental Science and Technology 34, 5084–5091. https://doi.org/10.1021/es001339o

Rivas, I., Beddows, D.C.S., Amato, F., Green, D.C., Järvi, L., Hueglin, C., Reche, C., Timonen, H., Fuller, G.W., Niemi, J. V., Pérez, N., Aurela, M., Hopke, P.K., Alastuey, A., Kulmala, M., Harrison, R.M., Querol, X., Kelly, F.J., 2020. Source apportionment of particle number size distribution in urban background and traffic stations in four European cities. Environment international 135, 105345. https://doi.org/10.1016/j.envint.2019.105345

Sawidis, T., Breuste, J., Mitrovic, M., Pavlovic, P., Tsigaridas, K., 2011. Trees as bioindicator of heavy metal pollution in three European cities. Environmental Pollution 159, 3560–70. https://doi.org/10.1016/j.envpol.2011.08.008

Scapellato, M.L., Lotti, M., 2007. Short-Term Effects of Particulate Matter: An Inflammatory Mechanism? Critical Reviews in Toxicology 37, 461–487. https://doi.org/10.1080/10408440701385622

Schwarze, P.E., Øvrevik, J., Låg, M., Refsnes, M., Nafstad, P., Hetland, R.B., Dybing, E., 2006. Particulate matter properties and health effects: Consistency of epidemiological and toxicological studies. Human and Experimental Toxicology 25, 559-579. https://doi.org/10.1177/096032706072520

Sgrigna, G., Baldacchini, C., Esposito, R., Calandrelli, R., Tiwary, A., Calfapietra, C., 2016. Characterization of leaf-level particulate matter for an industrial city using electron microscopy and X-ray microanalysis. Science of the Total Environment 548–549, 91–99. https://doi.org/10.1016/j.scitotenv.2016.01.057

Shi, J., Zhang, G., An, H., Yin, W., Xia, X., 2017. Quantifying the particulate matter accumulation on leaf surfaces of urban plants in Beijing, China. Atmospheric Pollution Research 8, 836–842. https://doi.org/10.1016/j.apr.2017.01.011

Subramanian, R., Donahue, N.M., Bernardo-Bricker, A., Rogge, W.F., Robinson, A.L., 2007. Insights into the primary-secondary and regional-local contributions to organic aerosol and PM2.5 mass in Pittsburgh, Pennsylvania. Atmospheric Environment 41, 7414–7433. https://doi.org/10.1016/j.atmosenv.2007.05.058

Terzano, C., Di Stefano, F., Conti, V., Graziani, E., Petroianni, A., 2010. Air pollution ultrafine particles: Toxicity beyond the lung. European review for medical and pharmacological sciences 14, 809–21.

Van Dingenen, R., Raes, F., Putaud, J.P., Baltensperger, U., Charron, A., Facchini, M.C., Decesari, S., Fuzzi, S., Gehrig, R., Hansson, H.C., Harrison, R., Hüglin, C., Jones, A.M., Laj, P., Lorbeer, G., Maenhaut, W., Palmgren, F., Quass, U., Rodriguez, S., Schneider, J., Ten Brink, H., Tunved, P., Tørseth, K., Wehner, B., Weingartner, E., Wiedensohler, A., Wåhlin, P., 2004. A European aerosol phenomenology - 1: Physical characteristics of particulate matter at kerbside, urban, rural and background sites in Europe. Atmospheric Environment 38, 2561–2577. https://doi.org/10.1016/j.atmosenv.2004.01.040

Vercauteren, J., Matheeussen, C., Wauters, E., Roekens, E., van Grieken, R., Krata, A., Makarovska, Y., Maenhaut, W., Chi, X., Geypens, B., 2011. Chemkar PM10: An extensive look at the local differences in chemical composition of PM10 in Flanders, Belgium. Atmospheric Environment 45, 108–116. https://doi.org/10.1016/j.atmosenv.2010.09.040

Viana, M., Kuhlbusch, T.A.J., Querol, X., Alastuey, a., Harrison, R.M., Hopke, P.K., Winiwarter, W., Vallius, M., Szidat, S., Prévôt, a. S.H., Hueglin, C., Bloemen, H., Wåhlin, P., Vecchi, R., Miranda, a. I., Kasper-Giebl, a., Maenhaut, W., Hitzenberger, R., 2008. Source apportionment of particulate matter in Europe: A review of methods and results. Journal of Aerosol Science 39, 827–849. https://doi.org/10.1016/j.jaerosci.2008.05.007

VMM, 2017. Luchtkwaliteit in het Vlaamse Gewest. Jaarverslag Immissiemeetnetten – 2016 (in Dutch). www.vmm.be/publicaties/luchtkwaliteit-in-het-vlaamse-gewest-2016.

Wang, L., Gong, H., Liao, W., Wang, Z., 2015. Accumulation of particles on the surface of leaves during leaf expansion. Science of the Total Environment 532, 420–434. https://doi.org/10.1016/j.scitotenv.2015.06.014

Weber, F., Kowarik, I., Säumel, I., 2014. Herbaceous plants as filters: Immobilization of particulates along urban street corridors. Environmental pollution (Barking, Essex : 1987) 186, 234–40. https://doi.org/10.1016/j.envpol.2013.12.011

WHO, 2015. www.who.int/gho/urban_health/situation_trends/urban_population_growth/. Accessed 28 September 2018.

WHO, 2016. Ambient air pollution: A global assessment of exposure and burden of disease. ISBN 9789241511353. World Health Organization.

WHO, 2018. www.who.int/news-room/detail/02-05-2018-9-out-of-10-people-worldwide-breathe-polluted-air-but-more-countries-are-taking-action. Accessed 25 March 2020.

Xie, R.K., Seip, H.M., Leinum, J.R., Winje, T., Xiao, J.S., 2005. Chemical characterization of individual particles (PM10) from ambient air in Guiyang City, China. Science of the Total Environment 343, 261–272. https://doi.org/10.1016/J.SCITOTENV.2004.10.012

Zhang, C., Qiao, Q., Appel, E., Huang, B., 2012. Discriminating sources of anthropogenic heavy metals in urban street dusts using magnetic and chemical methods. Journal of Geochemical Exploration 119–120, 60–75. https://doi.org/10.1016/j.gexplo.2012.06.014

Zhou, W., Apkarian, R.P., Wang, Z.L., Joy, D., 2006. Fundamentals of Scanning Electron Microscopy (SEM). In: Scanning Microscopy for Nanotechnology. Springer, New York, pp. 1–40. https://doi.org/10.1007/978-0-387-39620-0_1